Nanoscale

COMMUNICATION

View Article Online
View Journal | View Issue

Cite this: *Nanoscale*, 2014, **6**, 12440

Received 25th June 2014,
Accepted 9th September 2014

DOI: 10.1039/c4nr03550j

www.rsc.org/nanoscale

Superatom–atom super-bonding in metallic clusters: a new look to the mystery of an Au_{20} pyramid†

Longjiu Cheng,*[a] Xiuzhen Zhang,[a] Baokang Jin[a] and Jinlong Yang*[b]

Using the super valence bond model, a generalized chemical picture for the electronic shells of an Au_{20} pyramid is given. It is found that Au_{20} can be viewed to be a superatomic molecule, of which its superatomic 16c–16e core (T) is in D^3S hybridization bonded with four vertical Au atoms for the molecule-like (TAu_4) electronic shell-closure. Based on such a superatom–atom bonding model, TX_4 (X = F, Cl, or Br) are predicted to be very stable. Such a superatom–atom T–Au/T–X bonding enriches the scope of chemistry.

Au has the strongest relativistic effects among all elements, which results in strong sd hybridization and unique properties compared to other coin metals.[1] Small Au clusters display unique planar structures at about N = 2–10,[2] a transition from 2D to 3D structures at N = 11–13,[3] flat cage at N = 14–19,[4] pyramidal cage for Au_{20},[5] tubular structure for Au_{26},[6] golden fullerene for Au_{32} and Au_{72},[7,8] and core–shell structure at N = 33–38.[9]

Among the Au clusters, the Au_{20} cluster is very unique and possesses a pyramidal structure (T_d), which is far from spherical.[5] It has a remarkably large energy gap (1.77 eV) between the highest occupied and lowest unoccupied molecular orbitals (HOMO–LUMO), which is even larger than that of C_{60} (1.57 eV).[10] The large energy gap of the Au_{20} cage suggests that it is a highly inert and stable molecule and may have novel optical and catalytic properties.[11]

The stability of metallic clusters is mainly determined by the electronic structure rather than the atomic structure at a small size, which can be understood by the jellium model. The jellium model[12] assumes a uniform background of positive charge of the atomic nuclei of cluster and the innermost electrons, in which the valence electrons move and are subjected to an external potential. Therefore, the whole cluster can be viewed as a "superatom", and the appropriate aufbau rule for the super shells of spherical alkali–metal clusters is $|1S^2|1P^6|1D^{10}2S^2|1F^{14}2P^6|$ ... (Here the upper letters represent the super shells and the lower letters represent the electronic shells of atoms). Based on such a superatomic shell model, exceptional stability is associated with the magic numbers 2, 8, 20, 40 ..., which is in good agreement with the observed experimental abundance of alkali–metal clusters in the gas phase, and the magic stability of the icosahedral Al_{13}^- cluster.[13,14]

For Au ($5d^{10}6s^1$) clusters, the full-filled 5d electrons are mainly localized as lone-pairs (LPs) and $6s^1$ are free valence electrons. Due to the 6s character, the appropriate aufbau rule for the super shells of spherical Au clusters is $|1S^2|1P^6|1D^{10}|2S^21F^{14}|2P^61G^{18}|$ ..., associated with magic numbers 2, 8, 18, 34, 58, ...[15] The superatom theory has achieved great success in the stability of many experimentally produced thiolate-protected gold nanoparticles, which can be understood by the magic numbers, such as $Au_{102}(SR)_{44}$ (58e),[16] $Au_{68}(SR)_{34}$ (34e),[17] $Au_{44}(SR)_{28}^{2-}$ (18e),[18] $Au_{25}(SR)_{18}^-$ (8e),[19] and $Au_{12}(SR)_9^+$ (2e).[20] The large energy gap of the Au_{34} cluster viewed in experiments is also in agreement with the superatom shell model.[21]

However, the above superatom aufbau rule is based on a spherical field associated with spherical cluster motifs. The shell orders for non-spherical clusters may not follow the superatom aufbau rule. For example, the shell orders and magic numbers are much different in the ellipsoidal shell model.[22] Pyramidal Au_{20} is not at all spherical, of which the 20 valence electrons disagree with the magic numbers in the spherical jellium shell model.

To understand the magic stability of the Au_{20} cage, King *et al.*[23] thought that the 20 free electrons can be used to form a four-center-two-electron (4c–2e) bond in each of the 10 tetrahedral cavities of the Au_{20} cluster (four at vertices and six at

[a]*Department of Chemistry, Anhui University, Hefei, Anhui 230039, People's Republic of China. E-mail: clj@ustc.edu*

[b]*Hefei National Laboratory for Physics Sciences at the Microscale, University of Science & Technology of China, Hefei, Anhui 230026, People's Republic of China. E-mail: jlyang@ustc.edu.cn*

†Electronic supplementary information (ESI) available: Computational details, AdNDP chemical bonding of ten 10c–2e bonds of Au_{20}, and optimized structures of TM_4 and TX_4, low-lying isomers of TAu_4, and geometries of T^{4+}, T^{4-}, T^{2-}, $[Cu@T]^-$ and $[Cu@T]^{3-}$. See DOI: 10.1039/c4nr03550j

edges). Later, such a conjugated 4c–2e bonding model[24] was confirmed by natural bonding orbital (NBO) analysis using the adaptive natural density partitioning (AdNDP)[25,26] method (see Fig. s1 in ESI†).

Recently, we had proposed a super valence bond (SVB) model[27] to explain the electronic stability of the non-spherical shells of metallic clusters. In the SVB model, a non-spherical metallic cluster can be viewed as a superatomic molecule bonded by several spherical superatoms, of which the atomic nuclei can be shared by neighboring superatoms. The valence electrons are mainly delocalized over the region of each superatom instead of the whole cluster volume, following the rule of the jellium model. The superatoms can be open-shell, and molecule-like shell-closure is achieved by sharing the electron pairs between the superatoms *via* super bonding. Based on the SVB model, the electronic stability of lithium clusters[27] and ligand-protected Au clusters[28] can be understood by superatom–superatom super bonding.

To reveal the mystery of Au_{20}, we provide a new physical insight into the electronic structure of Au_{20} using the SVB model. As shown in Fig. 1a, the truncated tetrahedron Au_{16} core of the Au_{20} pyramid is sufficiently spherical, and can be viewed as an open-shell 16e-superatom (abbreviated as T). The electronic shells of T ($1S^21P^61D^8$) follow the rule of the spherical jellium model. Molecule-like electronic shell-closure is achieved by four superatom–atom super bonding (T–Au), and Au_{20} can be viewed as the superatomic molecule TAu_4. Fig. 1b gives a schematic representation of the bonding pattern of TAu_4. The $1S^21P^6$ shells of T are super LPs of the inner core. The five 1D orbitals split into two sets in a tetrahedral field: a set of lower double-degenerate orbitals ($1D_{x^2-y^2,z^2}$) and a set of higher triple-degenerate orbitals ($1D_{xy,yz,zx}$). The lower two $1D_{x^2-y^2,z^2}$ orbitals are fully-filled as super LPs. The higher three $1D_{xy,yz,zx}$ orbitals are in D^3S hybridization with the 2S orbital. The four D^3S super orbitals are bonded with the four $6s^1$ orbitals of the vertex Au atoms, splitting into four occupied lower bonding orbitals and four higher anti-bonding orbitals. Such a bonding pattern is analogous to the simple molecule OsH_4, where Os [$5s^25p^6(5d6s)^8$] is in d^3s hybridization bonded with four H atoms.

To verify the superatom–atom super bonding in Au_{20} (TAu_4), the molecular orbital (MO) and chemical bonding analysis are given by density function theory (DFT) calculations. The generalized gradient approximation method by Tao–Perdew–Staroverov–Scuseria (GGA-TPSS),[29] with relativistic effective core potential basis set (LanL2DZ) is adopted in this study. The calculated energy gap of Au_{20} under TPSS/LanL2DZ is 1.90 eV, which is in good agreement with the experimental value (1.77 eV).[5]

Fig. 2 compares the canonical Kohn–Sham MO diagrams of TAu_4 and OsH_4. As expected, the electronic configurations and orbital shapes of TAu_4 are in good agreement with those of OsH_4. $(1a_1)^2$ and $(1t_2)^6$ MOs correspond to the 1S and 1P (5s and 5p) orbitals of T (Os). The $(1e)^4$ MOs corresponds to $1D_{x^2-y^2,z^2}$ ($5d_{x^2-y^2,z^2}$) orbitals of T (Os). The $(2a_1)^2(2t_2)^6$ MOs correspond to the four D^3S-6s (d^3s-1s) T–Au (Os–H) bonding orbitals. The four anti-bonding D^3S-6s (d^3s-1s) MOs are $(3t_2)^0(3a_1)^0$ for T–Au and $(4t_2)^0(3a_1)^0$ for Os–H.

Chemical bonding analysis by AdNDP gives a more straightforward evidence for the superatom–atom bonding. As shown in Fig. 3a, the AdNDP analysis reveals six 16c–2e super LPs of T (super 1S, $1P_{x,y,z}$, $1D_{x^2-y^2,z^2}$) and four 17c–2e T–Au super σ-bonds in Au_{20}. This type of a bonding framework of TAu_4 is analogous to that of OsH_4, In particular between the shapes of the T–Au (D^3S-s) and Os–H (d^3s-s) bonds (Fig. 3b). Moreover, the occupancy numbers (ONs) of the super LPs and T–Au super bonds are very close to the ideal value 2.0 |e| (ON > 1.98 |e|), indicating a very high reliability.

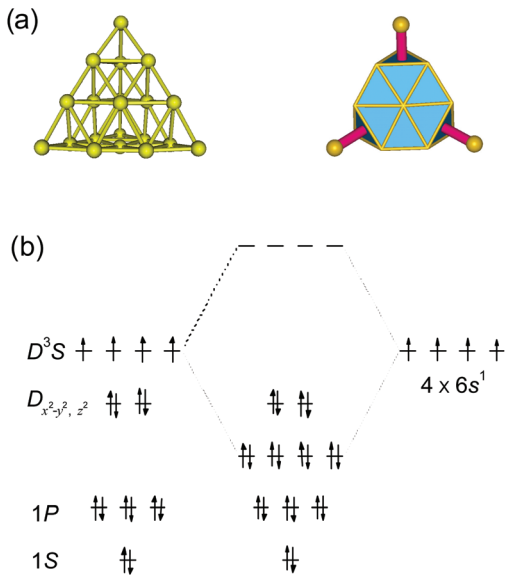

Fig. 1 (a) Structure and superatomic-molecule models of Au_{20} (TAu_4). (b) Schematic representation for the superatom–atom D^3S-s bonding of Au_{20} (TAu_4).

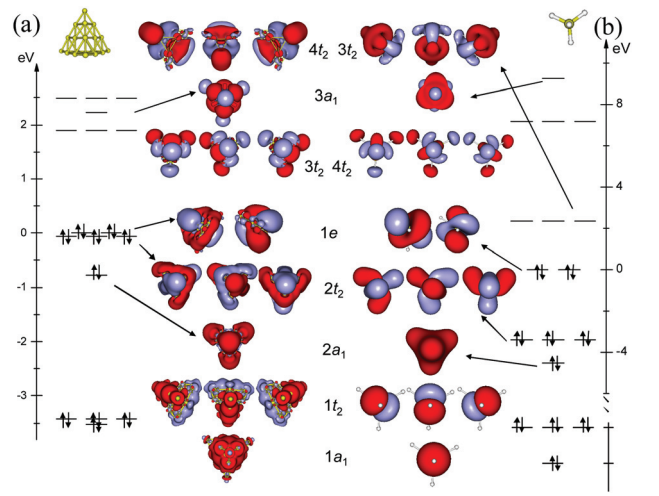

Fig. 2 Comparison of the Kohn–Sham MO diagrams of (a) Au_{20} (TAu_4) and (b) OsH_4.

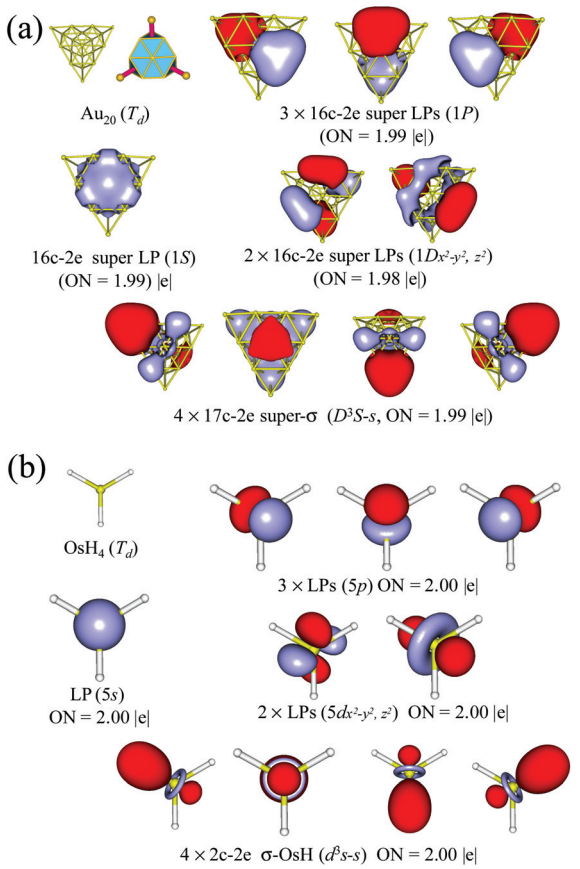

Fig. 3 Structures and AdNDP localized natural bonding orbitals of (a) Au_{20} (TAu_4) and (b) OsH_4.

In the formation of hybrid atomic orbitals, the atom is viewed as a point, and it is structure-free. However, the superatom has a 3D structure, and structural rearrangement may take place during the formation of hybrid super orbitals. As shown in Fig. 4, the lowest-energy structure of Au_{16} is a C_{2v} flat cage[4] in the singlet state ($^1A_1$). The singlet truncated tetrahedron remains a hollow T_d cage with a minor distortion (D_{2d}) due to the Jahn–Teller effect,[30] and is 0.49 eV higher in energy. After D^3S hybridization before the formation of the T–Au bonds, the quintet truncated tetrahedron retains the exact T_d symmetry without Jahn–Teller distortion and the hybridization energy is only 0.69 eV. Comparatively, the quintet state is even 2.15 eV higher in energy than the singlet state for the flat cage structure. In the Au_{20} (TAu_4) pyramid, the symmetry of geometry satisfies the symmetry of hybrid super orbitals, which may be the reason for its magic stability.

The four vertical Au atoms in Au_{20} can be replaced by other 1e-atoms. IA (H, Li, Na, and K) and other IB (Cu and Ag) elements can also form stable $Au_{16}M_4$ (TM_4) superatomic molecules with reasonably large HOMO–LUMO gaps and vertical ionic potentials (VIPs) (see Fig. s2 in ESI†). In TM_4 superatomic molecules, T acts as a Lewis base in the −4 charge state.

Based on the VB theory, Os atoms can act as a Lewis acid and bond with four halogens to form stable OsX_4 compounds. Similarly, T(IV) should also act as a Lewis acid and TX_4 should be a stable compound. As expected, TX_4 compounds (X = F, Cl, Br, OH, SH or CN) were calculated to be very stable with large HOMO–LUMO gaps and VIPs (see Fig. s3 in ESI†). The AdNDP analysis shows that the electronic configuration of T in TX_4 is similar to that in TM_4, where T is also in D^3S hybridization bonded with four p_z orbitals of X. Taking TCl_4 as an example, Fig. 5a plots the four AdNDP localized super T–Cl bonds (D^3S-$3p_z$), which are obviously similar to the Os–Cl bonds (d^3s-$3p_z$) of $OsCl_4$ in the orbital shapes (Fig. 5b).

The reaction energies of 4/5 Au_{20} + 2 X_2 → TX_4 are calculated to be very large: F(−7.70 eV) > Cl(−5.29 eV) > Br(−4.89 eV), which indicates that TX_4 is thermally more stable than bare Au_{20}. Moreover, TF_4 is the most stable and T(IV) acts as a very hard Lewis acid. Thus, the chemical properties of T are very different from that of the Au element which often acts as a soft Lewis acid.

The predicted TM_4 and TX_4 superatomic molecules are real local minima in the potential energy surface (PES), verified by the absence of imaginary vibrational modes. Are these

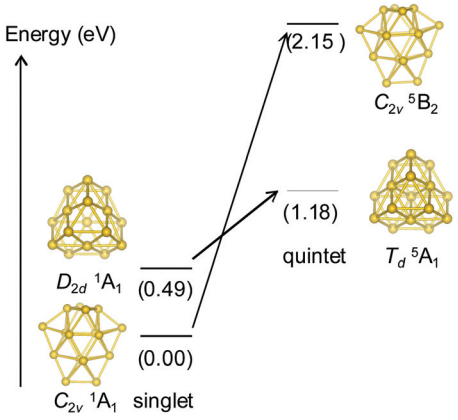

Fig. 4 Energy levels of the singlet and quintet states of the flat cage and truncated tetrahedron motifs of Au_{16}.

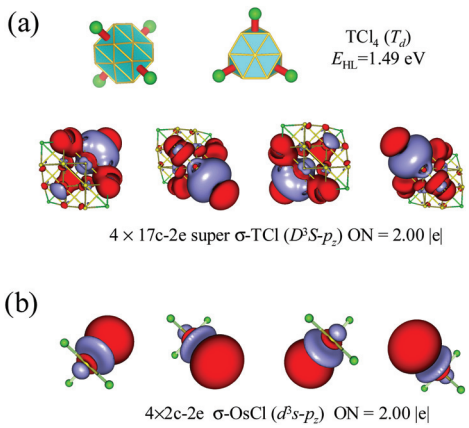

Fig. 5 (a) Superatomic-molecule models and four AdNDP localized super T–Cl bonds of $Au_{16}Cl_4$ (TCl_4), and (b) four AdNDP localized Os–Cl bonds of $OsCl_4$.

molecules the global minima in PES? Taking $Au_{16}Cl_4$ as a test case, we performed an unbiased global minimum search of the PES using the method of genetic algorithm plus density functional theory. In the global search, over 600 minima are relaxed by DFT. The TCl_4 superatomic molecule is successfully located in the unbiased search as the global minimum one and is 0.49 eV lower in energy than that of the second isomer (see Fig. S4 in ESI†).

The T–Au super bond in TAu_4 is almost nonpolar. The NBO analysis reveals that the polarity of the T–Au bond is about 51%:49%. However, other T–M and T–X bonds may have greater polarities. The polarity of T–Na and T–Cl bonds are 93%:7% and 15%:85%, respectively. Therefore, TNa_4 can be viewed as $T^{4-}{\cdot}4Na^+$ and TCl_4 as $T^{4+}{\cdot}4Cl^+$, where the T–Na and T–Cl super bonds are mainly ionic and T is a Lewis acid in the former and a Lewis base in the latter. T^{4-} may be the global minimum structure, and is 1.14 eV lower in energy than the −4 ion of the C_{2v} flat cage. However, T^{4+} is 0.10 eV higher in energy than the +4 ion of the C_{2v} structure. The bare T^{4+} and T^{4-} ions are not as stable as in the compounds, where the calculated HOMO–LUMO gaps are only 0.92 eV and 1.10 eV, respectively, much lower than those of $T^{4+}{\cdot}4Cl^+$ (1.49 eV) and $T^{4-}{\cdot}4Na^+$ (1.61 eV). This is due to the D^3S hybridization of T, which is significantly stabilized in the tetrahedral field of $4Cl^+$ or $4Na^+$. The geometry of the 3D superatoms should satisfy the hybridization of superatomic orbitals differently from the orbital hybridization of atoms, where each atom is taken as a 0D point. Thus, T is a magic number tetravalent superatom in a tetrahedral geometry instead of spherical in the tetrahedral coordination with D^3S hybridization.

It is noticeable that 20e is the magic number of sodium clusters in the spherical jellium model. However, the magic number is 18e for Au clusters due to its 6s character, where $[Cu@Au_{16}]^-$ and $Zn@Au_{16}$ are viewed as 18e close-shell superatoms.[31] Evidences can be given from the geometries of T^{4+}, T^{4-} and T^{2-}. T^{4+} and T^{4-} maintain the tetrahedral geometry in TAu_4, however, T^{2-} tends to be a spherical cage due to the spherical jellium effect of 18e. Moreover, the HOMO–LUMO gap of the spherical 20e $[Cu@Au_{16}]^{3-}$ (0.73 eV) is also much lower than that of the spherical 18e $[Cu@Au_{16}]^-$ (1.21 eV), indicating an 18e shell closure (all are shown in Fig. S4 in ESI†). Thus, the magic electronic stability of TAu4 is due to the superatom–atom bonding instead of the spherical jellium effect.

In summary, we investigate the electronic structure of the Au_{20} cage (T_d) based on the recently proposed SVB model. Au_{20} is proven to be a superatomic molecule (TAu_4) bonded by one 16c–16e Au_{16} superatom and four Au atoms, and it is an exact analogue of OsH_4 molecule. Clear evidences for the T–Au superatom–atom super bonding are given by comparing the MO diagrams and AdNDP bonding patterns of TAu_4 and OsH_4. Moreover, based on our model, TX_4 (X = F, Cl, Br, OH, SH or CN) are predicted to be very stable, where T(IV) acts as a hard Lewis acid different from the chemical property of the Au element. we conclude that this type of superatom–atom super bonding gives a new physical insight in chemical bonding and enriches the scopes of chemistry, and new molecules/compounds and materials can be designed based on this type of superatom–atom super bonding.

It is a pleasure to thank professor Boldyrev for the AdNDP codes. This work is financed by the National Natural Science Foundation of China (21121003, 21273008, 91021004), by the National Key Basic Research Program of China (2011CB921404), and by the 211 Project of Anhui University.

Notes and references

1 (*a*) H. Hakkinen, M. Moseler and U. Landman, *Phys. Rev. Lett.*, 2002, **89**, 033401; (*b*) Y. Pei and X. Zeng, *Nanoscale*, 2012, **4**, 4054; (*c*) R. Jin, *Nanoscale*, 2010, **2**, 343; (*d*) H. Hakkinen, *Nat. Chem.*, 2012, **4**, 443; (*e*) H. Qian, M. Zhu, Z. Wu and R. Jin, *Acc. Chem. Res.*, 2012, **45**, 1470; (*f*) D. Jiang, *Nanoscale*, 2013, **5**, 7149.

2 (*a*) G. Mills, M. Gordon and H. Metiu, *Chem. Phys. Lett.*, 2002, **359**, 493; (*b*) P. Pyykko, *Chem. Soc. Rev.*, 2008, **37**, 967; (*c*) H. De, S. Krishnamurty, D. Mishra and S. Pal, *J. Phys. Chem. C*, 2011, **115**, 7278; (*d*) R. Olson, S. Varganov, M. Gordon, H. Metiu, S. Chretien, P. Piecuch, K. Kowalski, S. Kucharski and M. Musial, *J. Am. Chem. Soc.*, 2005, **127**, 1049.

3 (*a*) K. Spivey, J. Williams and L. Wang, *Chem. Phys. Lett.*, 2006, **432**, 163; (*b*) M. Gruber, G. Heimel, L. Romaner, J. Bredas and E. Zojer, *Phys. Rev. B: Condens. Matter*, 2008, **77**, 165411.

4 (*a*) S. Bulusu and X. Zeng, *J. Chem. Phys.*, 2006, **125**, 154303; (*b*) P. Gruene, D. Rayner, B. Redlich, A. van der Meer, J. Lyon, G. Meijer and A. Fielicke, *Science*, 2008, **321**, 674; (*c*) Y. Gao, N. Shao, Y. Pei, Z. Chen and X. Zeng, *ACS Nano*, 2011, **5**, 7818.

5 J. Li, X. Li, H. J. Zhai and L. Wang, *Science*, 2003, **299**, 864.

6 W. Fa and J. Dong, *J. Chem. Phys.*, 2006, **124**, 114310.

7 (*a*) M. Johansson, D. Sundholm and J. Vaara, *Angew. Chem., Int. Ed.*, 2004, **43**, 2678; (*b*) X. Gu, M. Ji, S. Wei and X. Gong, *Phys. Rev. B: Condens. Matter*, 2004, **70**, 205401.

8 A. Karttunen, M. Linnolahti, T. Pakkanen and P. Pyykkö, *Chem. Commun.*, 2008, 465.

9 N. Shao, W. Huang, Y. Gao, L. Wang, X. Li, L. Wang and X. Zeng, *J. Am. Chem. Soc.*, 2010, **132**, 6596.

10 (*a*) H. Kroto, J. Heath, S. O'Brien, R. Curl and R. Smalley, *Nature*, 1985, **318**, 162; (*b*) W. Krätschmer, L. Lamb, K. Fostiropoulos and D. Huffman, *Nature*, 1990, **347**, 354; (*c*) X. Wang, C. Ding and L. Wang, *J. Chem. Phys.*, 1999, **110**, 8217.

11 (*a*) W. Huang, S. Bulusu, R. Pal, X. Zeng and L. Wang, *ACS Nano*, 2009, **3**, 1225; (*b*) K. Wu, J. Li and C. Lin, *Chem. Phys. Lett.*, 2004, **388**, 353; (*c*) Y. Gao, S. Bulusu and X. Zeng, *J. Am. Chem. Soc.*, 2005, **127**, 15680; (*d*) X. Zhang, M. Guo, D. Wu, P. Liu, Y. Sun, L. Zhang and F. Fan, *J. Inorg. Organomet. Polym.*, 2011, **21**, 758; (*e*) K. Bobuatong, S. Karanjit, R. Fukuda, M. Ehara and H. Sakurai, *Phys. Chem. Chem. Phys.*, 2012, **14**, 3103.

12 (*a*) W. Knight, K. Clemenger, W. de Heer, W. Saunders, M. Chou and M. Cohen, *Phys. Rev. Lett.*, 1984, **52**, 2141; (*b*) W. de Heer, *Rev. Mod. Phys.*, 1993, **65**, 611.
13 R. Leuchtner, A. Harms and A. Castleman Jr., *J. Chem. Phys.*, 1989, **91**, 2753.
14 (*a*) D. Bergeron, A. Castleman Jr., T. Morisato and S. Khanna, *Science*, 2004, **304**, 84; (*b*) D. Bergeron, P. Roach, A. Castleman Jr., N. Jones and S. Khanna, *Science*, 2005, **307**, 231.
15 M. Walter, J. Akola, O. Lopez-Acevedo, P. Jadzinsky, G. Calero, C. Ackerson, R. Whetten, H. Gronbeck and H. Hakkinen, *Proc. Natl. Acad. Sci. U. S. A.*, 2008, **105**, 9157.
16 P. Jadzinsky, G. Calero, C. Ackerson, D. Bushnell and R. Kornberg, *Science*, 2007, **318**, 430.
17 A. Dass, *J. Am. Chem. Soc.*, 2009, **131**, 11666.
18 R. Price and R. Whetten, *J. Am. Chem. Soc.*, 2005, **127**, 13750.
19 (*a*) M. Heaven, A. Dass, P. White, K. Holt and R. Murray, *J. Am. Chem. Soc.*, 2008, **130**, 3754; (*b*) M. Zhu, C. Aikens, F. Hollander, G. Schatz and R. Jin, *J. Am. Chem. Soc.*, 2008, **130**, 5883.
20 Y. Zhang, S. Shuang, C. Dong, C. Lo, M. Paau and M. Choi, *Anal. Chem.*, 2009, **81**, 1676.
21 (*a*) A. Lechtken, D. Schooss, J. Stairs, M. Blom, F. Furche, N. Morgner, O. Kostko, B. Issendorff and M. Kappes, *Angew. Chem., Int. Ed.*, 2007, **46**, 2944; (*b*) X. Gu, S. Bulusu, X. Li, X. Zeng, J. Li, X. Gong and L. Wang, *J. Phys. Chem. C*, 2007, **111**, 8228.
22 K. Clemenger, *Phys. Rev. B: Condens. Matter*, 1985, **32**, 1359.
23 R. King, Z. Chen and P. Schleyer, *Inorg. Chem.*, 2004, **43**, 4564.
24 D. Zubarev and A. Boldyrev, *J. Phys. Chem. A*, 2009, **113**, 866.
25 D. Zubarev and A. Boldyrev, *Phys. Chem. Chem. Phys.*, 2008, **10**, 5207.
26 (*a*) D. Zubarev and A. Boldyrev, *J. Org. Chem.*, 2008, **73**, 9251; (*b*) A. Sergeeva, D. Zubarev, H. Zhai, A. Boldyrev and L. Wang, *J. Am. Chem. Soc.*, 2008, **130**, 7244; (*c*) W. Huang, A. Sergeeva, H. Zhai, B. Averkiev, L. Wang and A. Boldyrev, *Nat. Chem.*, 2010, **2**, 202; (*d*) L. Cheng, *J. Chem. Phys.*, 2012, **136**, 104301; (*e*) L. Li and L. Cheng, *J. Chem. Phys.*, 2013, **138**, 094312; (*f*) A. Sergeeva, Z. Piazza, C. Romanescu, W. Li, A. Boldyrev and L. Wang, *J. Am. Chem. Soc.*, 2012, **134**, 18065; (*g*) L. Cheng, Y. Yuan, X. Zhang and J. Yang, *Angew. Chem., Int. Ed.*, 2013, **1021**, 144.
27 L. Cheng and J. Yang, *J. Chem. Phys.*, 2013, **138**, 141101.
28 (*a*) L. Cheng, C. Ren, X. Zhang and J. Yang, *Nanoscale*, 2013, **5**, 1475; (*b*) Y. Yuan, L. Cheng and J. Yang, *J. Phys. Chem. C*, 2013, **117**, 13276.
29 J. Tao, J. Perdew, V. Staroverov and G. Scuseria, *Phys. Rev. Lett.*, 2003, **91**, 146401.
30 G. Chen, Q. Wang, Q. Sun, Y. Kawazoe and P. Jena, *J. Chem. Phys.*, 2010, **132**, 194306.
31 (*a*) L. Wang, S. Bulusu, H. Zhai, X. Zeng and L. Wang, *Angew. Chem., Int. Ed.*, 2007, **46**, 2915; (*b*) L. Wang, R. Pal, W. Huang, X. Zeng and L. Wang, *J. Chem. Phys.*, 2009, **130**, 051101.